Arsenite-Induced Aryl Hydrocarbon Receptor Nuclear Translocation Results in Additive Induction of Phase I Genes and Synergistic Induction of Phase II Genes

Simone Kann,[1] Ming-ya Huang, Cameron Estes, John F. Reichard, Maureen A. Sartor, Ying Xia, and Alvaro Puga

Center for Environmental Genetics and Department of Environmental Health, University of Cincinnati Medical Center, Cincinnati, Ohio

ABSTRACT

Complex mixtures of carcinogenic metalloids, such as arsenic, and polycyclic aromatic hydrocarbons or halogenated aromatic hydrocarbons are common environmental contaminants. The biological consequences of exposure to these mixtures are unpredictable and, although the health effects of individual chemicals may be known, the toxicity of environmental mixtures is largely unexplored. Arsenic, not a potent mutagen by itself, is co-mutagenic with many DNA-damaging agents. Mixtures of arsenite plus benzo[a]pyrene (B[a]P) augment B[a]P mutagenicity, suggesting that arsenite might uncouple expression of phase I and II genes responsible for detoxification. We have studied the effects of arsenite exposure on the activation of the aryl hydrocarbon receptor (AHR) and its subsequent role in gene transactivation. Treatment of mouse Hepa-1 cells with arsenite induces AHR nuclear translocation and binding to the Cyp1a1 gene promoter with the same efficiency as tetrachlorodibenzo-p-dioxin (TCDD), the most potent ligand of the AHR; however, TCDD and B[a]P are an order of magnitude more potent than arsenite in up-regulating Cyp1a1 transcription. Global profiling analyses of cells treated with arsenite plus B[a]P indicate that several phase I and II detoxification genes are in some cases additively and in others synergistically de-regulated by the mixtures. Real-time reverse transcription-polymerase chain reaction analyses of mouse embryonic fibroblasts showed that the mixtures had an additive effect on the mRNA levels of Cyp1b1, a prototypical phase I detoxification gene, and an AHR-dependent synergistic effect on the corresponding levels of Nqo1, a prototypical phase II gene. We conclude that exposure to arsenite/B[a]P mixtures causes regulatory changes in the expression of detoxification genes that ultimately affect the metabolic activation and disposition of toxicants.

One of the current problems in toxicology is the lack of information on the health effects of complex chemical mixtures. Data are scarce, and the task of reproducing every possible complex mixture of toxicants to analyze its effects would be Herculean. However, environmental exposures to toxic or carcinogenic compounds rarely result from the presence of a single, isolated toxic agent. Complex mixtures often include a combination of metals and PAHs. Of these, arsenic and B[a]P, respectively, remain among the most frequent mixtures in the environment and are found among the top 20 hazardous substances in the Agency for Toxic Substances and Disease Registry/Environmental Protection Agency priority list (http://www.atsdr.cdc.gov/cxcx3.html). Of more than 9000 Superfund sites where PAHs are major contaminants, a full 50% have also arsenic as a cocontaminant.

Arsenic, a known carcinogen, is most commonly found in the environment as arsenate (As^{5+}), although arsenite (As^{3+}) is the most toxic and the most likely carcinogenic species in humans (Tinwell et al., 1991). Arsenic consistently fails to show carcinogenic effects in rodent models unless it is used at very high doses (Wang and Rossman, 1996). The initial observation that arsenic was co-mutagenic with ultraviolet light led to the concept that arsenic carcinogenicity

ABBREVIATIONS: PAH, polycyclic aromatic hydrocarbons; B[a]P, benzo[a]pyrene; AHR, aryl hydrocarbon receptor; ARNT, aryl hydrocarbon receptor nuclear translocator; MEF, mouse embryonic fibroblasts; DMSO, dimethyl sulfoxide; 3M4NF, 3′-methoxy-4′-nitroflavone; PBS, phosphate-buffered saline; PBST, phosphate-buffered saline/Tween 20; HSP90, 90-kDa heat-shock protein; PCR, polymerase chain reaction; RT, reverse transcription; bp, base pair(s); EMSA, electrophoretic mobility shift assay; MG-132, N-benzoyloxycarbonyl (Z)-Leu-Leu-leucinal; TGF, transforming growth factor; TBHQ, tert-butylhydroquinone; TCDD, tetrachlorodibenzo-p-dioxin.

MOLECULAR PHARMACOLOGY

resulted from the activation of genes that enhanced the effect of the primary carcinogen (Wang and Rossman, 1996). Using gene arrays, arsenite as been shown to be a potent deregulator of gene expression, particularly of genes involved in oxidative stress responses (Andrew et al., 2003; Rea et al., 2003). The ability of arsenite to bind to and oxidize vicinal dithiols within a protein or to bridge two thiols between two proteins has suggested the possibility that one of the mechanisms of gene inactivation by arsenic may involve the oxidation of transcription factors and protein kinases with vicinal thiols, such as those found in zinc-finger transactivators, and the ensuing changes in the ability of the oxidized factors to function (Wang and Rossman, 1996). This concept was proven correct at least for the inactivation of nuclear factor κB activity by the reaction of arsenite with critical cysteines in the Ikβ-kinases (Kapahi et al., 2000; Roussel and Barchowsky, 2000).

The Ah receptor (AHR) is a ligand-activated basic region-helix-loop-helix/periodicity-aryl hydrocarbon receptor nuclear translocator-simple-minded (Per-ARNT-Sim) transcription factor that forms heterodimers with ARNT and binds to *cis*-acting AHR response element enhancer elements in the regulatory domains of target genes, such as the cytochrome P450 *Cyp1a1* and the NAD(P)H-dependent quinone oxidoreductase *Nqo1,* leading to changes in chromatin structure and activation of gene transcription. The role of non-AHR ligands as modifiers of AHR-dependent responses has been much less well studied than the role of ligands, such as B[*a*]P or TCDD, in the toxic responses that they induce. Recent reports have demonstrated that modification of Ah receptor-dependent gene expression can result from oxidative stress, suggesting that coexposure to receptor ligands and pro-oxidant environmental pollutants could disrupt the coordinate regulation of detoxification genes. The precise step in the AHR signaling pathway that is acted upon by oxidative stress is not clear. Sulfhydryl modifying agents have been shown to block binding of TCDD to the AHR (Denison et al., 1987; Kester and Gasiewicz, 1987) and binding of AHR to DNA (Ireland et al., 1995), suggesting that AHR activation may be directly regulated by redox changes. In addition, H_2O_2 has been shown to inhibit *Cyp1a1* inducibility, although this effect may be mediated through transcription factors other than the AHR (Barker et al., 1994; Morel and Barouki, 1998; Xu and Pasco, 1998).

The ability of arsenic and other metals and metalloids to generate oxidative stress has been extensively investigated (Stohs and Bagchi, 1995; Nieboer and Fletcher, 1996), but their potential to modify AHR-dependent gene expression and to modulate the toxicity of AHR ligands such as B[*a*]P is almost unknown. Our previous results have shown that low concentrations of sodium arsenite had a strong synergistic effect in the genotoxicity of B[*a*]P, an effect that required CYP1A1-dependent metabolism (Maier et al., 2002). These results suggested the possibility that the combined exposure to arsenite and B[*a*]P might disrupt the regulatory mechanisms that control transcription from B[*a*]P-inducible gene promoters and cause an uncoupling of phase I and II gene expression with a concomitant imbalance in B[*a*]P metabolism. We have tested this hypothesis by studying the effects of arsenite exposure on the activation of the AHR and its subsequent role in the transactivation of phase I and II genes. We find that treatment of mouse hepatoma Hepa-1

cells with arsenite induces AHR nuclear translocation and binding to the *Cyp1a1* gene promoter with the same efficiency as TCDD, its most potent ligand; however, TCDD and B[*a*]P up-regulate *Cyp1a1* transcription to a much greater extent than arsenite. In contrast, global profiling and real-time RT-PCR analyses of gene expression indicate that several phase II detoxification genes are in some cases additively and in others synergistically deregulated by arsenite plus B[*a*]P treatment.

Materials and Methods

Cell Culture and Chemical Treatments. Cells known to respond to a B[*a*]P or TCCD challenge by activation of the AHR include the mouse hepatoma Hepa-1c1c7 cell line (Bernhard et al., 1973) and MEFs from $Ahr^{+/+}$ C57BL/6J mice (Tan et al., 2002). MEFs from $Ahr^{-/-}$ mice (Fernandez-Salguero et al., 1995) do not transactivate detoxification genes after a TCDD or a B[*a*]P challenge (Tan et al., 2002). MEFs were prepared by standard techniques from 14.5-day-old embryos and were grown in α-minimal essential medium (Invitrogen, Carlsbad, CA) supplemented with 5% fetal bovine serum, 100 μg/ml penicillin, and 100 μg/ml streptomycin. Treatments were applied when the cells were at 80 to 90% confluence. Sodium arsenite was freshly dissolved at 1000× strength in sterile deionized water before use. TCDD and B[*a*]P were added to the cells dissolved in DMSO at concentrations of 5 nM and 5 μM, respectively. Control cells received an equal volume of DMSO or ethanol, never to exceed a final concentration of 0.1% in the cell cultures. *tert*-Butylhydroquinone was dissolved in sterile deionized water and used at 25 μM. The AHR antagonist 3M4NF (Nazarenko et al., 2001), a gift from Dr. Thomas Gasiewicz (University of Rochester Medical Center, Rochester, NY), was dissolved in DMSO and used at 1 μM.

Immunofluorescence Staining. Cells grown on cover glasses were fixed for 15 min with 3.7% paraformaldehyde in PBS, washed with PBS three times, permeabilized, and reacted at 30°C for 1 h with an affinity-purified rabbit anti-AHR raised in our laboratory against an N-terminal peptide of the mouse AHR. These antibodies were affinity-purified with the peptide immunogen and showed specificities against AHR proteins similar to those of proteins commercially available from BIOMOL Research Laboratories (Plymouth Meeting, PA) and those that were a generous gift from Dr. Richard Pollenz (University of South Florida, Tampa, FL). This was followed by staining with a rhodamine-labeled goat anti-rabbit IgG in the presence of 1 mg/ml of the DNA dye bisbenzimide Hoechst 33258 for 30 min. Fluorescence was visualized using a Zeiss fluorescence microscope. A total of 5 to 10 fields were evaluated for each treatment group.

Electrophoretic Mobility Shift Assays. Nuclear extracts were prepared by procedures described previously (Puga et al., 2000) with minor modifications. Cells were washed twice with ice-cold PBS, harvested by scraping, and collected by centrifugation. Pelleted cells were resuspended in 100 mM NaCl, 20 mM Tris-HCl pH 8.0, 1 mM EDTA, 10 μg/ml aprotinin, 10 μg/ml leupeptin, 1 mM phenylmethylsulfonyl fluoride, 0.1 mM $NaVO_4$, 10 mM NaF, 10 mM NaP_2O_7, 0.5% Nonidet P-40 and lysed for 5 min on ice and homogenized with 20 strokes of a loose-fitting Dounce homogenizer. Nuclei were pelleted at low speed and nuclear extracts were obtained in a final volume of 100 μl of a buffer containing 2 mM EDTA, 2 mM dithiothreitol, 0.4 M KCl, 10% glycerol and 25 mM HEPES, pH 7.9, at a protein concentration of 10–20 μg /μl. DNA-binding reactions were performed in a 20-μl reaction volume with 10,000 dpm (approximately 0.1 ng) of double-stranded AHR response element probe (Puga et al., 2000) and 5 - 15 μg nuclear protein, in a buffer containing 1 mM EDTA, 1 mM dithiothreitol, 80 mM KCl, 10% glycerol, 1 μg poly(dI-dC)-poly(dI-dC) carrier, and 20 mM HEPES, pH 7.8. One strand of each complementary pair of oligonucleotides was end-labeled with T4 polynucleotide kinase and [γ-^{32}P]ATP and annealed

to an excess of the unlabeled complementary oligonucleotide. Binding reactions were allowed to proceed for 20 min at room temperature and samples were loaded onto nondenaturing 4% polyacrylamide gels. After electrophoresis at 200 V for 2 to 3 h in 0.5× Tris-borate buffer, the gels were dehydrated and exposed to X-ray film.

Western Blot Analysis. To prepare nuclear extracts for immunoblotting the above protocol was modified such that the final nuclei pellets were resuspended in lysis buffer and briefly sonicated to disrupt the nuclei. Debris was removed by centrifugation at 12,000 rpm for 15 min. Protein concentration of the supernatants was determined, and the supernatants were stored at −80°C until ready to use. Ten micrograms of protein were resolved by electrophoresis in 7% SDS-polyacrylamide gels and transferred to nitrocellulose membranes. Membranes were blocked with 5% low-fat milk in PBST (0.1 M PBS with 0.1% Tween 20) and incubated for 1 h at room temperature with the appropriate primary antibody at 1:1000 to 1:5000 dilution in PBST containing 3% BSA. In addition to the anti-AHR, anti-HSP90 (Santa Cruz Biotechnology, Santa Cruz, CA) was also used. After washing the blots with PBST, the membrane was incubated for 1 h in 1:10,000 goat anti-rabbit HRP-conjugated antibody (Santa Cruz) in PBST containing 5% milk. After washing, bands were visualized using PicoWest Chemiluminescent Super Signal (Pierce, Rockford, IL). The same procedure was used for detection of β-actin using and anti-β-actin antibody generously provided by Dr. James L. Lessard (Cincinnati Children's Hospital Medical Center, Cincinnati, OH).

RNA Isolation and Real-Time RT-PCR. Total RNA was isolated using Tri Reagent (Invitrogen) according to the manufacturer's instructions with additional purification steps applied to RNA samples used for microarray analysis. To verify RNA quality before labeling for microarray analyses, samples were analyzed using a 2100 Bioanalyzer (Agilent Technologies, Palo Alto, CA). cDNA was synthesized by reverse transcription of 20 μg of total RNA in a total volume of 30 μl containing 1× reverse transcriptase buffer, 2.5 μM random hexamers, 0.25 mM dNTP, 0.01 M dithiothreitol, 20 U of RNAsin, and 200 U of SuperScript II RNase H⁻ reverse transcriptase (Invitrogen). Samples were incubated at 42°C for 1 h, and the reverse transcriptase was inactivated by heating to 99°C for 5 min. For real-time PCR amplification, 3 μl of cDNA were amplified with mouse Cyp1a1 primers 5′-GCCTTCATTCTGGAGACCTTCC-3′ and 5′-CAATGGTCTCTCCGATGC-3′, giving a product of 280 bp. Amplification of Cyp1b1 was with primers 5′-AAGGAAGGGGAGTGC-GATAG-3′ and 5′-ATGGGGGAGATAGGAGGAAAGG-3′, giving a product of 227 bp. Amplification of Nqo1 cDNA was with primers 5′-ACCCCACTCTATTTTGCTCC-3′ and 5′-ACTTACTCCTTTTC-CCATCCTC-3′, giving a product size of 279 bp. β-Actin amplification of the same cDNA samples was used as an internal standard. Amplification was conducted in the Smart Cycler (Cepheid, Sunnyvale, CA) in a total volume of 25 μl consisting of 1× Brilliant SYBR Green QPCR Master Mix (Stratagene, La Jolla, CA) and 0.4 μM primers. The reaction mixtures were heated to 95°C for 10 min and immediately cycled 40 times through a 24-s denaturing step at 95°C, a 60-s annealing step at 55°C and a 46-s elongation step at 72°C. Cycle threshold of each sample was automatically determined to be the first cycle at which a significant increase in optical signal above an arbitrary baseline set at 30 fluorescence units was detected. All determinations were done in triplicate. The values shown represent the cycle threshold ratios of experimental to control cells treated with DMSO, normalized to the β-actin mRNA level in the same sample.

Fluorescent Labeling of Target cDNAs and High-Density Microarray Hybridization. Total RNA was isolated using Tri Reagent (Invitrogen) according to the manufacturer's instructions with additional purification steps applied to RNA samples used for microarray analysis. To verify RNA quality before labeling for microarray analyses, samples were analyzed using an Agilent 2100 Bioanalyzer. Labeling of cDNAs, preparation of microarrays, and

hybridization reactions were performed by the University of Cincinnati Functional Genomics Core and are briefly described here. Fluorescence-labeled cDNAs were synthesized from 20 μg of total RNA using an indirect amino allyl labeling method (DeRisi et al., 1996). The cDNA was synthesized by an oligo(dT)-primed, reverse transcriptase reaction, and the cDNA was labeled with monofunctional reactive cytidine-3 and cytidine-5 dyes (Cy3 and Cy5; Amersham Biosciences, Piscataway, NJ). Specific details of the labeling protocols may be found at http://microarray.uc.edu.

The hybridization probes were from arrayed mouse oligonucleotide microarrays derived from the Operon/Qiagen Verified Libraries containing 13,332 sequences from annotated mouse genes, affixed each in a 100-μm diameter spot to polylysine-treated microscope slides. The hybridization targets were the paired Cy3- and Cy5-labeled control and test cDNAs, which were mixed in approximately equal proportions and applied to the microarray for hybridization under high-stringency conditions. After hybridization and washing unhybridized targets, Cy3 (green) and Cy5 (red) fluorescent channels were simultaneously scanned with independent lasers at 10-μm resolution. Each comparison was done in duplicate with flipped dye arrays to allow for the removal of gene-specific dye effects.

Data Analysis and Normalization. Microarray hybridization data representing raw spot intensities generated by the GenePix software were analyzed to identify differentially expressed genes under different experimental conditions. Data normalization was performed in three steps for each microarray separately. First, channel-specific local background intensities were subtracted from the median intensity of each channel (Cy3 and Cy5). Second, background-adjusted intensities were log-transformed and the differences (R) and averages (A) of log-transformed values were calculated as $R = \log_2(X1) - \log_2(X2)$ and $A = [\log_2(X1) + \log_2(X2)]/2$, where $X1$ and $X2$ denote the Cy5 and Cy3 intensities after subtracting local backgrounds, respectively. Third, data centering was performed by fitting the array-specific local regression model of R as a function of A (Dudoit et al., 2002). The difference between the observed log-ratio and the corresponding fitted value represented the normalized log-transformed gene expression ratio. Normalized log intensities for the two channels were then calculated by adding half of the normalized ratio to A for the Cy5 channel and subtracting half of the normalized ratio from A for the Cy3 channel.

Identification of Differentially Expressed Genes. The statistical analysis was performed for each gene separately by fitting the following mixed effects linear model (Wolfinger et al., 2001): $Y_{ijk} = \mu + A_i + S_j + C_k + Y_{ijk}$, where Y_{ijk} corresponds to the normalized log-intensity on the ith array ($i = 1, \ldots, 15$), with the jth treatment combination ($j = 1, \ldots, 5$), and labeled with the kth dye (k = 1 for Cy5, and 2 for Cy3). μ is the overall mean log-intensity, A_i is the effect of the ith array, S_j is the effect of the jth treatment combination and C_k is the effect of the kth dye. Assumptions about model parameters were the same as described elsewhere (Wolfinger et al., 2001), with array effects assumed to be random and treatment and dye effects assumed to be fixed. Statistical significance of the differential expression between different treatment combinations, after adjusting for the array and dye effects, was assessed by calculating p values for corresponding linear contrasts. Multiple-hypothesis testing adjustment was performed by calculating false discovery rate values (Benjamini and Hochberg, 1995; Reiner et al., 2003). Cut-off for significantly deregulated genes was set at a ratio of two above or below control values and, for all the genes presented in Table 1, the false discovery rate was <0.1. Data normalization and statistical analyses were performed using SAS (SAS Institute Inc., Cary, North Carolina). Gene ontology annotations were extracted from the National Center for Bioinformatics web site (http://www.ncbi.nlm.nih.gov/RefSeq/).

Cytotoxicity Determinations. Cytotoxicity of arsenic was determined by measuring lactic dehydrogenase release from treated cells, as described previously (Maier et al., 2000). No significant cytotoxicity was observed by concentrations of arsenite of 25 μM and

TABLE 1
Genes deregulated by arsenite, B[*a*]P, or both
Positive values indicate -fold increases; negative values indicate -fold decreases.

Accession	Symbol	Gene name	B[*a*]P	As	B[*a*]P + As	GO Process	GO Function
U12785	Aldh3a1	Aldehyde dehydrogenase-3A1	6.7	2.0	14.7	Oxidative metabolism	Aldehyde dehydrogenase activity
U12961	Nqo1	NAD(P)H quinone oxidoreductase-1	4.6	2.0	9.2	Electron transport	Oxidoreductase
X56824	Hmox1	Heme oxygenase-1	1.7	11.4	20.5	Heme oxidation	Oxidoreductase
M35021	Hspa1b	Heat shock protein, 70 kDa 1	1.2	2.7	5.7	Heat shock response. Anti-apoptosis	ATP binding during oxidative stress
M12571	Hspa1a	Heat shock protein, 70 kDa 3	1.2	2.6	5.1	Protein folding	ATP binding during oxidative stress
AJ404467	Dnmt3l	DNA (cytosine-5-)-methyltransferase 3-like	−1.4	4.8	5.1	Methylation imprinting	Protein binding
U95053	Gclm	Glutamate-cysteine ligase modulatory subunit	1.7	2.1	4.5	Glutathione biosynthesis	Glutamate-cysteine ligase
U85498	Gclc	Glutamate-cysteine ligase catalytic subunit	1.8	2.4	2.7	Glutathione biosynthesis	Glutamate-cysteine ligase
U95607	Dnajb3	Heat shock protein 40, DNAJ-homolog	1.5	2.0	2.7	Heat shock response	ATP binding during oxidative stress
L07577	Hsb1	Heat shock protein, 25 kDa	1.5	2.1	2.7	Heat shock response. Anti-apoptosis	ATP binding during oxidative stress
L26163	Hist1h1e	Histone H1e	1.4	2.3	2.5	Nucleosome spacing	DNA binding
J05149	Insr	Insulin receptor	−1.1	2.1	2.1	Insulin receptor signaling	Protein kinase activity
AB027565	Txnrd1	Thioredoxin reductase 1	1.1	2.2	2.2	Electron transport	Oxidoreductase
AF185613	Gpc1	Glypican 1	5.2	1.3	5.8	Unknown	Extracellular matrix
D30782	Ereg	Epiregulin	2.2	1.8	3.4	Cell cycle regulation	Growth factor activity
AB009694	Maff	V-MAF fibrosarcoma oncogene	2.9	1.0	3.0	Regulation of transcription	DNA binding
X67644	Ier3	Immediate early response 3	2.0	−1.0	2.7	Regulation of cell death	Integral to membrane
U03283	Cyp1b1	Cytochrome P450, 1b1, benz[*a*]anthracene inducible	2.4	−1.4	2.4	Electron transport	Monooxygenase activity
BC003897	Arl6ip5	ADP-ribosylation-like factor 6 interacting protein 5	2.1	1.1	2.3	Glutamate transport	Protein binding
M88242	Ptgs2	Prostaglandin-endoperoxide synthase 2	2.3	−1.8	2.1	Prostaglandin biosynthesis	Cyclooxygenase activity
U23921	Osp94	Osmotic stress protein	1.5	1.4	4.5	Protein folding	ATP binding during oxidative stress
AB025408	Esd	Esterase 10	1.5	1.6	2.9	Unknown	Carboxylesterase
U40930	Sqstm1	Sequestosome-1	1.3	1.7	2.5	Transcription cofactor	Binds to ubiquitin. Oxidative stress
K02236	Mt2	Metallothionein 2	1.4	1.6	2.1	Metal homeostasis	Metal ion binding
NM_013541	Gstp1	Glutathione S-transferase, pi 2	1.4	1.9	2.0	Detoxification	Glutathione transferase
X15378	Mpo	Myeloperoxidase	−1.3	−1.7	−2.0	Oxidative stress response	Oxidoreductase
M33960	Pai1	Plasminogen activator inhibitor 1. Serpine 1	−2.3	−2.0	−2.0	Regulation of angiogenesis	Endopeptidase inhibitor
NM_010444	Nr4a1	Nuclear receptor subfamily 4, group A, member 1	−2.3	−2.6	−3.5	Inhibition of caspase activation	Nuclear receptor
X69620	Inhbb	Inhibin beta-B	1.2	−2.4	−2.0	Cell growth and differentiation	Growth factor activity
M87276	Thbs1	Thrombospondin 1	−1.9	−2.3	−2.1	Cell adhesion	Calcium ion binding
AF118855	Tprt	trans-Prenyltransferase	−1.6	−2.3	−2.2	Unknown	Transferase
NM_025711	Aspn	Asporin	1.2	−2.1	−2.3	Extracellular matrix	Small molecule transport
NM_010512	Igf1	Insulin-like growth factor 1	1.2	−2.8	−2.5	Anti-apoptosis	Growth factor activity
U25096	Klf2	Kruppel-like factor 2 (lung)	−1.2	−2.0	−2.5	Transcription regulation	DNA binding
D50411	Adam12	A disintegrin and metalloproteinase domain 12 (meltrin α)	−1.3	−2.1	−2.6	Cell adhesion, extracellular matrix	Metallopeptidase
NM_172053	Adamts16	A disintegrin-like and metalloprotease (reprolysin type)	−1.3	−2.0	−2.6	Integrin-mediated signaling	Metallopeptidase
X98014	Siat8E	Sialyltransferase 8E	−1.8	−2.2	−4.2	Protein glycosylation	Sialyltransferase
U52524	Has2	Hyaluronan synthase 2	−1.5	−2.4	−4.3	Protein glycosylation	Transferase
AB024923	Sgcd	Sarcoglycan, delta (dystrophin-associated glycoprotein)	−2.0	1.0	−2.0	Cytoskeleton organization	Protein binding
X85999	Il1rap	Interleukin 1 receptor accessory protein	−2.3	−1.6	−2.1	Cytokine-mediated signaling	IL−1 receptor activity
U85713	Plcb1	Phospholipase Cb	−3.2	1.2	−2.1	Intracellular signaling	PI phospholipase
X95281	Dhrs	Retinal short-chain dehydrogenase/reductase 1	−2.4	−1.3	−2.4	Metabolism	Oxidoreductase
L09562	Ptprg	Protein tyrosine phosphatase, receptor type, G	−2.7	1.3	−2.5	Transmembrane signaling	Protein phosphatase
Z34524	Prkcm	Protein kinase C, μ	−2.4	−1.5	−2.5	Intracellular signaling	Protein kinase activity
Y18276	Nbea	Neurobeachin	−3.5	−1.8	−2.9	Protein targeting	Protein kinase A binding
X97817	Sema5a	Sema domain, seven thrombospondin repeats	−3.3	−1.1	−3.0	Receptor activity	Transmembrane signaling
AF033655	Pftk1	PFTAIRE protein kinase 1	−2.8	1.2	−3.1	Protein phosphorylation	Protein kinase
AF090696	Cugbp2	CUG triplet repeat, RNA-binding protein 2	−2.7	1.2	−3.1	mRNA splice factor	Splice site selection
D38417	Ahr	Aryl-hydrocarbon receptor	−2.9	1.1	−3.4	Cell cycle	Transcription factor

TABLE 1
Continued

Accession	Symbol	Gene name	B[a]P	As	B[a]P + As	GO Process	GO Function
NM_011160	*Prkg1*	Protein kinase, cGMP-dependent, type I	−2.8	−1.2	−3.9	Pprotein phosphorylation	cAMP-dependent signaling
X57413	*Tgfb2*	Transforming growth factor β-2	−2.1	−1.2	−4.2	Cell differentiation	Growth factor
X99572	*Figf*	C-fos induced PDGF family member	−1.2	−1.3	−2.0	Angiogenesis	Growth factor
Z29532	*Fst*	Follistatin	−1.2	−1.2	−2.0	Differentiation	BMP/TGFβ inhibitor
X69619	*Inhba*	Inhibin-bA	−1.2	−1.6	−2.0	Cell growth and differentiation	Growth factor activity
X62934	*Tacr1*	Tachykinin receptor 1	−1.1	−1.7	−2.0	G-protein signaling pathway	G-protein coupled receptor activity
AB024565	*Hs6s2*	Heparan sulfate 6-*O*-sulfotransferase 2	−1.3	−1.5	−2.0	Protein sulfation	Transferase
X66976	*Col8a1*	Procollagen, type VIII, α1	−1.8	−1.3	−2.0	Cell adhesion	Extracellular matrix
U31758	*Hdac2*	Histone deacetylase 2	−1.2	−1.1	−2.0	Chromatin remodeling	Histone deacetylase
X61455	*Napb*	*N*-Ethylmaleimide–sensitive attachment protein	−1.0	−1.2	−2.1	Transport	Intracellular transport
U79550	*Snai2*	Snail homolog	−1.4	−1.1	−2.1	Development	DNA binding
AF054623	*Fzd1*	Frizzled 1	−1.3	−1.3	−2.2	Receptor signaling	G-protein-coupled receptor activity
U89924	*Ppp31r3c*	Protein phosphatase 1 inhibitory subunit	−1.3	−1.4	−2.2	Glycogen metabolism	Protein phosphatase
AF117709	*Sfrp4*	Secreted frizzled-related protein 4	−1.3	−1.2	−2.5	Receptor signaling	G-protein-coupled receptor activity
AF038507	*Cip7*	RIKEN cDNA 2010204K13 gene	−1.3	−1.5	−2.5	Unknown	Unknown

below for up to 24 h after treatment. This is also clearly evident in the fluorescent micrographs in the figures.

Results

Arsenite Induces AHR Nuclear Translocation. To test the hypothesis that combined exposures to arsenic and B[a]P could disrupt expression of phase I and II detoxification genes, we studied potential effects of arsenite exposure on AHR activation. To this effect, we measured changes in cellular compartmentalization of the AHR in mouse hepatoma Hepa-1 cells after exposure to increasing doses of sodium arsenite using immunocytochemistry, Western immunoblotting, and electrophoretic mobility shift assays. Immunocytochemistry with specific anti-AHR antibodies 90 min after treatment showed dose response effects on nuclear translocation. At low micromolar arsenite concentrations, between 3 and 6 μM, there was no difference between control cells and arsenite-treated cells, with the AHR showing cytoplasmic localization. At concentrations of 12 μM and higher, AHR localization became patently nuclear, an effect indistinguishable from that observed in the positive control cells treated with 5 nM TCDD (Fig. 1).

We chose the 12 μM arsenite concentration to do a time response analysis. Nuclear translocation was evident by 2 h and continued until 8 h, the last experimental determination, closely paralleling the time response of control cells treated with 5 nM TCDD (Fig. 2). By 8 h, however, both arsenite- and TCDD-treated cells showed a diffuse staining pattern, consistent with loss of AHR from the nucleus, as described elsewhere (Pollenz, 2002).

To confirm the above results at the biochemical level, we prepared nuclear extracts from arsenite-treated and control Hepa-1 cells and examined them for the presence of the AHR by immunoblotting and electrophoretic mobility shift assays. Western blots were more sensitive than immunocytochemistry, and dose-dependent AHR nuclear translocation was already detectable at the 6 μM dose and increased with dose (Fig. 3A). In time response experiments, nuclear translocation seemed to

proceed at a slower rate in arsenite-treated cells than in their TCDD-treated counterparts. Maximum accumulation took place at 2 to 4 h after arsenite treatment, whereas by 1 h, TCDD-treated cells shown maximum nuclear AHR levels (Fig. 3B). Down-regulation of nuclear AHR also seemed to be faster after TCDD treatment, with significant decreases by 4 h after treatment, whereas losses of nuclear AHR were not evident until 8 h after arsenite treatment (Fig. 3B).

Current evidence indicates that the totality of the cytosolic AHR complex translocates to the nucleus upon TCDD activation of the receptor, including the Hsp90 chaperone molecules (Pollenz, 2002). To determine whether arsenite-induced AHR nuclear translocation also extended to Hsp90, we used anti-Hsp90 antibodies in Western blots of the same nuclear extracts. Increases in the level of nuclear Hsp90 were found at 2, 4, and 8 h after TCDD but not after arsenite treatment (Fig. 3B), suggesting that arsenite-dependent translocation followed a molecular pathway different from the classic ligand-dependent pathway. Immunoblotting for β-actin confirmed that these results were not an artifact of gel loading differences. As further confirmation of these results, electrophoretic mobility shift assays showed dose-dependent increases in the DNA-binding activity of nuclear AHR complexes (Fig. 3C).

3M4NF is a flavonoid compound and AHR antagonist that blocks AHR nuclear translocation (Nazarenko et al., 2001). Immunocytochemistry and Western blot analysis of Hepa-1 cells showed inhibition of AHR nuclear translocation in controls simultaneously treated with TCDD and 3M4NF but not in cells treated with 3M4NF and arsenite (Fig. 4, A and B). These results strongly indicate that arsenite exposure causes the nuclear translocation of the AHR by mechanisms unlike those followed by ligands. At the least, the Hsp90 component of the chaperone complex does not seem to translocate with the AHR and translocation is not inhibited by 3M4NF.

AHR-Dependent Gene Expression Is Only Weakly Up-Regulated by Arsenite. To determine whether arsenite-mediated AHR nuclear translocation and DNA-binding activation resulted in gene transactivation, we measured the

induction of the cytochrome P450 *Cyp1a1* gene in Hepa-1 hepatoma cells after treatment with various concentrations of sodium arsenite and compared it with the effect of induction by 5 nM TCDD alone or in combination with the same concentrations of sodium arsenite. Total RNA was extracted from these cells, and Cyp1a1 mRNA levels were determined by real-time RT-PCR. Treatment with arsenite alone led to a weak induction of Cyp1a1, with low levels, in the range of 2- to 5-fold over control, but significantly different from vehicle-treated control cells (Fig. 5A). Treatment with TCDD induced Cyp1a1 by 35- to 40-fold, and combined treatment with TCDD and arsenite superinduced Cyp1a1 expression to levels significantly higher than those observed in cells treated with TCDD alone (Fig. 5A). These results confirm our previous conclusions that activation of the AHR by arsenite follows different molecular pathways than activation by TCDD, leading also to different outcomes in gene transactivation.

Low-Dose Gene Expression Effects of Arsenite. In an effort to identify low-concentration effects of arsenic, we examined the consequences of coexposures to arsenite plus B[*a*]P, which we have previously shown to be synergistically comutagenic (Maier et al., 2002). As measured by real-time RT-PCR, cotreatment of Hepa-1 cells with 2 μM sodium arsenite and 5 μM B[*a*]P did not cause a significant increase in Cyp1a1 induction relative to the effect of B[*a*]P alone. Arsenite by itself was responsible for not more than a doubling in Cyp1a1 mRNA levels, which was statistically significant compared with vehicle-treated control cells (Fig. 5B).

We also determined the effect of arsenic exposure on the induction of *Nqo1*, a prototypical phase II gene, by B[*a*]P. To
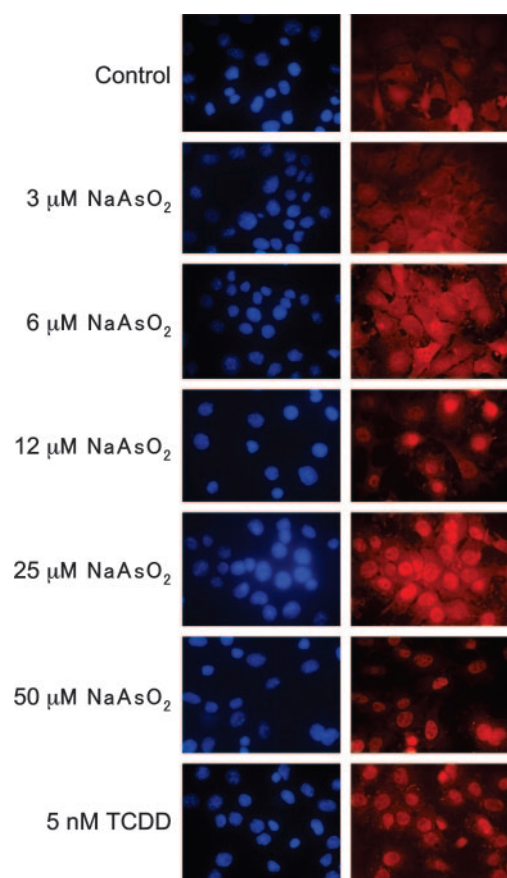
Fig. 1. Immunofluorescence microscopy of Hepa-1 cells treated with various concentrations of sodium arsenite. Cells were grown on cover glasses, treated for 90 min with the indicated concentrations of arsenite, fixed with 2% and reacted with an affinity-purified rabbit anti-AHR raised in our laboratory against an N-terminal peptide of the mouse AHR, followed by staining with a rhodamine-labeled goat anti-rabbit IgG in the presence of 1 mg/ml of the DNA dye bisbenzimide Hoescht 33258 for 30 min. Fluorescence was visualized using a Zeiss fluorescence microscope. Panels labeled "Control" and "5 nM TCDD" are negative and positive controls, respectively. The panels on the left show the Hoescht staining, and those on the right show the anti-AHR immunofluorescence; the identical fields are shown for both.
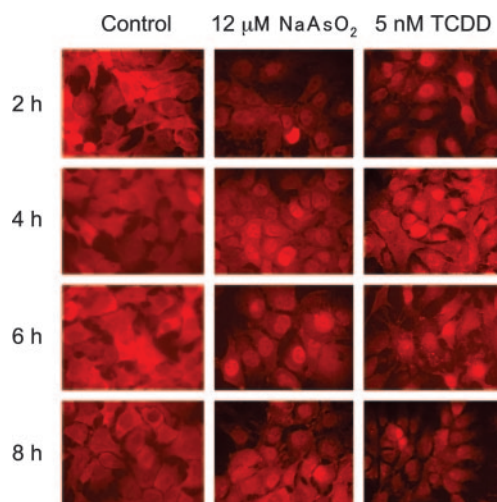
Fig. 2. Immunofluorescence microscopy of Hepa-1 cells treated with 12 μM arsenite or 5 nM TCDD for various lengths of time. Conditions and treatments were as described in Fig. 1, except that the cells were exposed to a single arsenite concentration for various lengths of time.
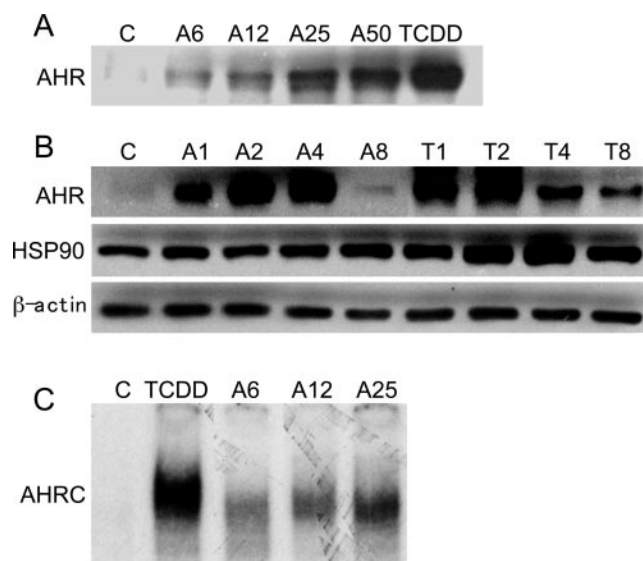

Fig. 3. Western blot and EMSA analyses of arsenite-induced AHR nuclear translocation. A, nuclear extracts from Hepa-1 cells treated for 1 h with the indicated micromolar concentrations of arsenite or with DMSO vehicle (*C*) or 5 nM TCDD were separated in polyacrylamide gels and the AHR detected with specific anti-AHR antibodies. B, nuclear extracts were prepared after time intervals of 1, 2, 4, and 8 h after treatment with 12 μM arsenite (lanes labeled A) or with 5 nM TCDD (lanes labeled T). Lane C is a nuclear extract from control DMSO-treated cells. The Western blot was probed with anti-AHR, anti-HSP90, and anti-actin antibodies, as indicated. C, AHR EMSA of nuclear extracts from Hepa-1cells treated for 1 h with increasing concentrations of arsenite. AHRC denotes the position of the AHR/ARNT DNA binding complex. Only the part of the gel relevant to AHR detection is shown.

insure that only primary effects of treatment were observed, cells we exposed only for 4 h to 2 μM sodium arsenite, 5 μM B[a]P, or to a combined mixtures of arsenite plus B[a]P. As control for the effect on *Nqo1*, we also treated cells with 25 μM TBHQ, a classic monofunctional phase II gene inducer, and with arsenite plus TBHQ. Treatment with B[a]P plus arsenite increased slightly Cyp1a1 induction above the level found in cells treated with B[a]P alone, although the difference was not statistically significant (Fig. 6). Arsenite alone, TBHQ, and the combination of TBHQ plus arsenite did not change Cyp1a1 mRNA levels (Fig. 6). The response of the *Nqo1* genes was very different. Arsenite increased by 2-fold Nqo1 mRNA over vehicle control, a change that was statistically significant, and, when used in combination, more than doubled the effect of B[a]P, an effect that was also statistically significant (Fig. 6). In contrast, *Nqo1* induction by TBHQ was not affected by arsenite (Fig. 6). These results suggested that the combination of arsenite and B[a]P had different regulatory consequences depending on the gene being measured and prompted us to use global gene expression profiling to investigate the extent of the response to combined treatments with these two agents.

Global Gene Expression Responses to Low Concentration Mixtures of Arsenite and B[a]P. To insure that the responses that we would observe in these experiments would not be caused by genetic abnormalities resulting from long-term maintenance of cells in culture, we used MEFs from C57BL/6J mice within five to six passages from establishment from 14.5-day-old fetuses. MEFs show Ah receptor-dependent responses similar to those of hepatocytes, although they tend to express CYP1B1 instead of CYP1A1 as the predominant cytochrome P450 (Alexander et al., 1997). Genes deregulated by either 2 μM arsenite, 5 μM B[a]P, or by

a mixture of the two, are shown in Table 1. Several genes involved in oxidative stress responses and glutathione metabolism were up-regulated by arsenic, whereas *Hmox1* and two phase II detoxification genes, *Aldh3a1* and *Nqo1*, were highly up-regulated by B[a]P and by the mixture, whereas a third-phase II gene, *Gstp*, was up-regulated only by the arsenite + B[a]P mixture. Genes involved in glutathione biosynthesis, such as *Gclm* and *Gclc*, and several genes coding for oxidoreductases were induced by arsenite or by arsenite + B[a]P mixtures, as were many heat-shock proteins, involved in antiapoptotic responses during oxidative stress. Among the genes deregulated by either arsenite or a mixture of B[a]P and arsenite, there is a large number of genes involved in TGF-β, integrin, cell adhesion, and extracellular matrix signaling processes, including *TGF-β2* itself, plasminogen activator inhibitor-1, inhibin-βA and inhibin-βB, thrombospondin-1, at least two *Adamt* genes, coding for disintegrin-like metalloproteinases and other genes involved in protein glycosylation. It seems that one of the major consequences of exposure to these mixtures is the up-regulation of
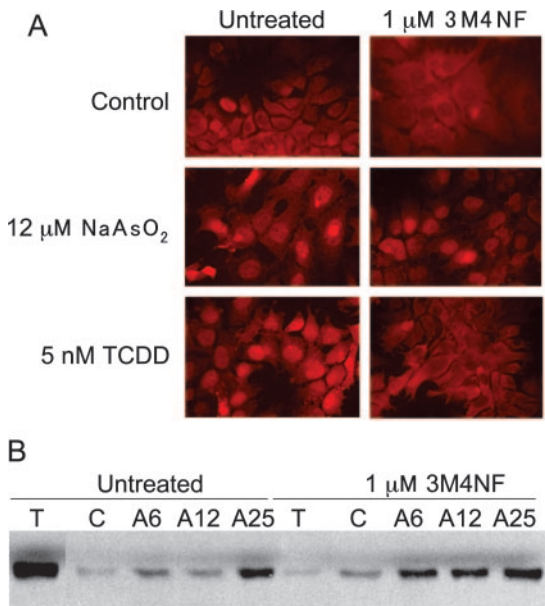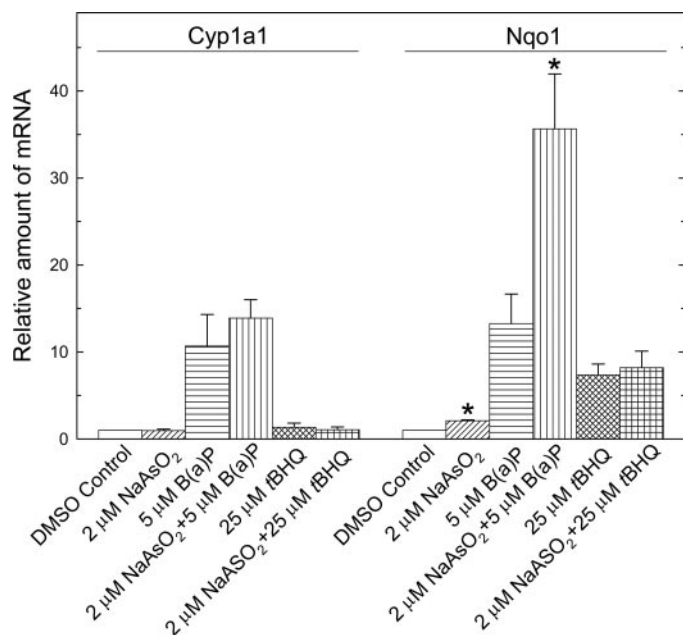

Fig. 4. 3M4NF does not inhibit arsenite-mediate AHR nuclear translocation. A, Hepa-1 cells were treated with 1 μM 3M4NF or DMSO control and either left untreated or treated with 12 μM sodium arsenite or 5 nM TCDD for 90 min. Thereafter, they were processed for AHR immunofluorescence as described in Fig. 1. B, nuclear protein extracts were prepared from DMSO- or 3M4NF-treated Hepa-1 cells cotreated with TCDD (*T*), arsenite at various micromolar concentrations (*A*) or nothing (*C*). The Western blot was probed with an anti-AHR antibody.
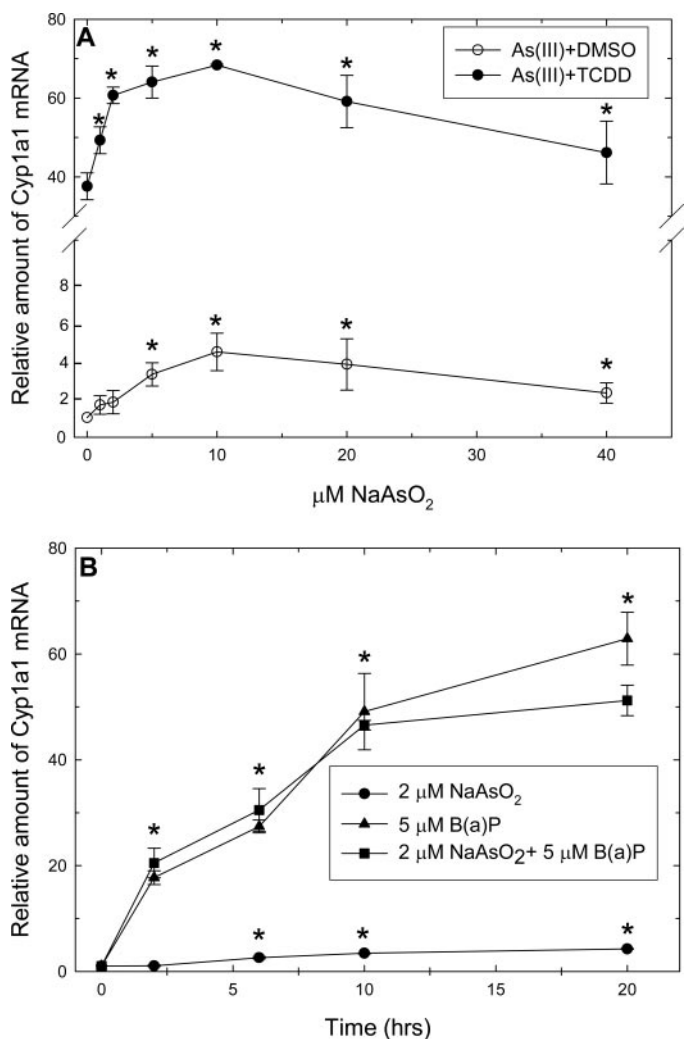
Fig. 5. Real-time RT-PCR detection of Cyp1a1 mRNA in Hepa-1 cells treated with arsenite or with arsenite and TCDD or arsenite with B[a]P. A, total RNA was extracted from cells treated with the concentrations of arsenite indicated in the abscissa in combination with DMSO vehicle or 5 nM TCDD. B, time course of Cyp1a1 induction after treatment with arsenite, B[a]P, or a combination of the two.

oxidative stress and protein chaperone responses and the down-regulation of the TGF-β pathway.
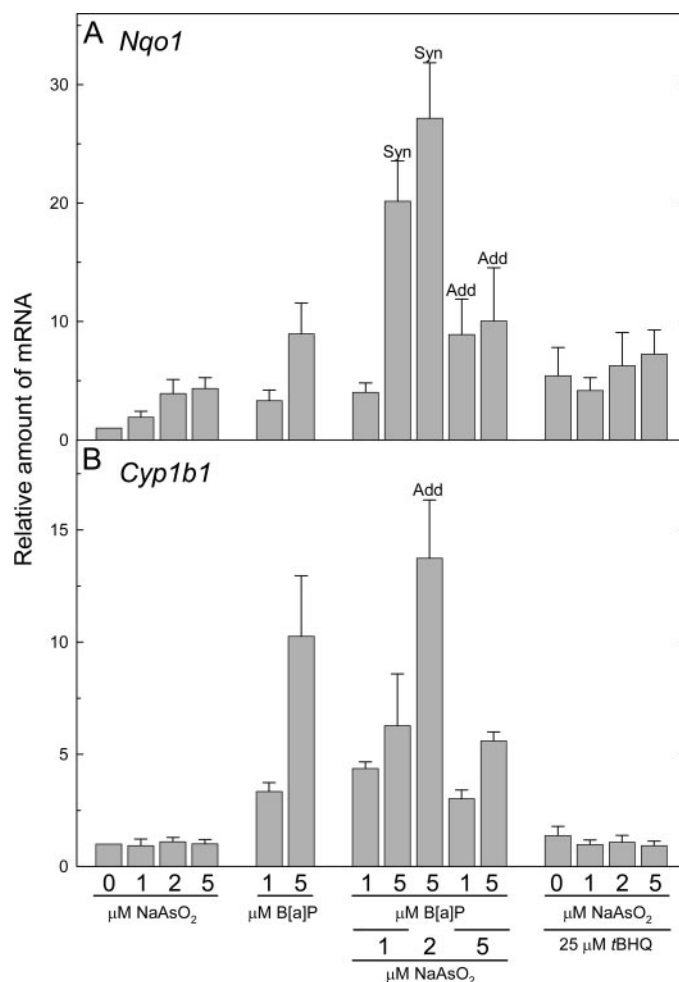
Synergistic and Additive Interactions of Arsenite and B[a]P in Gene Regulation. For some genes in Table 1, the mRNA levels of the cotreatments seem to show additive effects in some cases, synergistic in others, and no effect in yet others. For example, synergy is apparent for the phase II genes *Nqo1* and *Aldh3a1*, as well as for the oxidative stress sentinel—but not a phase II gene—*Hmox1*. In contrast, *Cyp1b1*, a prototypical phase I detoxification gene, shows no cooperative effects (Table 1). To verify the gene profiling data and characterize in more detail the apparent differences between phase I and II genes, we measured Nqo1 and Cyp1b1 mRNA levels by real-time RT-PCR after treatment of MEFs with various concentrations of sodium arsenite, B[a]P, or combinations of the two. Messenger RNA levels of Nqo1 increased with increasing concentrations of arsenite or B[a]P and showed a synergistic effect when the lower arsenite concentrations of 1 and 2 μM were combined with 5 μM B[a]P; however, at 5 μM arsenite, the effect was no longer synergistic, and became simply additive (Fig. 7A). There was also an observable effect of the mixture on Cyp1b1 mRNA levels, but the effect on this gene was additive, not synergistic, and was statistically significant only for the mixture of 2 μM arsenite plus 5 μM B[a]P. Surprisingly, mixtures of 1 or 5 μM arsenite plus 5 μM B[a]P gave rise to lower Cyp1b1 mRNA levels than 5 μM B[a]P alone (Fig. 7B). These effects seemed to be specific for the mixtures of arsenite and B[a]P, because mixtures of arsenite and the phase II inducer TBHQ did not show interactive effects in either *Nqo1* or *Cyp1b1* expression (Fig. 7, A and B). Synergy between arsenite and B[a]P in the induction of Nqo1 expression depended on the presence of a functional AHR, as demonstrated by the finding that it took place only in *Ahr*^{+/+} but not in *Ahr*^{−/−} MEFs (Fig. 8).

Discussion

The results presented in this article indicate that treatment of cultured mouse hepatoma cells with sodium arsenite induces the nuclear translocation of the Ah receptor in a dose-dependent manner. By 6 to 12 μM, translocation was clearly evident by immunofluorescence, Western immunodetection, and EMSA. AHR translocation was not competed by 3M4NF, an AHR antagonist, suggesting that arsenite-mediated translocation was not a ligand-dependent effect. Unlike ligand-dependent translocation, arsenite-dependent translocation led to a limited induction of *Cyp1a1* to levels 10-fold lower than those induced by TCDD but significantly different from controls. Arsenite + TCDD and arsenite + B[a]P had additive effects on the induction of *Cyp1a1* in Hepa-1 cells and of *Cyp1b1* in mouse MEFs, but the effect was synergistic and AHR-dependent for the induction of *Nqo1,* a phase II detoxification gene. Global gene profiling experiments with arsenite plus B[a]P mixtures showed the synergistic induction of several other phase II genes and of genes coding for
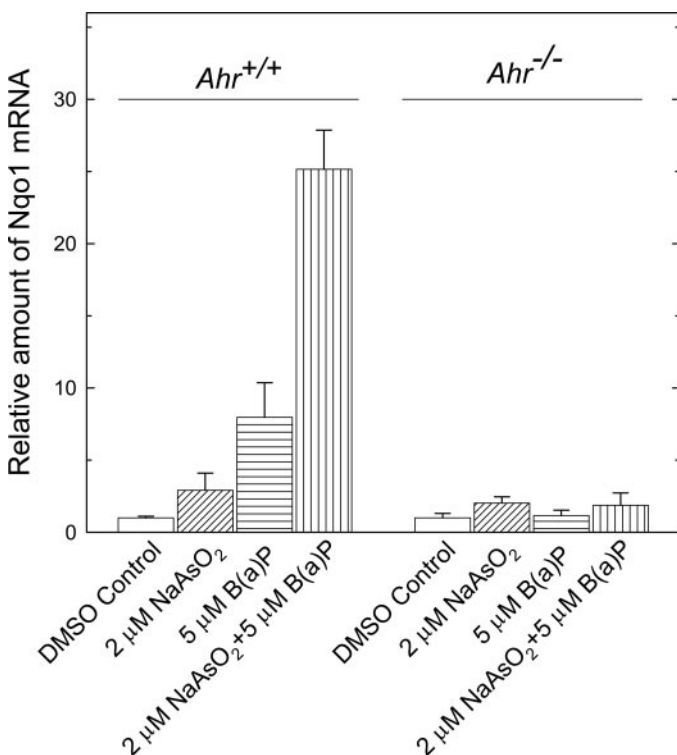
Fig. 6. Comparison of regulatory changes induced by a mixture of arsenite and B[a]P in the mRNA levels of Cyp1a1 and Nqo1. RNA from Hepa-1 cells treated for 6 h with the indicated concentrations of arsenite, B[a]P, and TBHQ, alone or in combination, was analyzed for the levels of Cyp1a1 and Nqo1.

Fig. 7. Effect of combined mixtures of arsenite, B[a]P, and TBHQ on the mRNA levels of Nqo1 (A) and Cyp1b1 (B) in mouse embryo fibroblasts. MEFs from C57BL/6J mice were treated for 6 h with the concentrations of arsenite, B[a]P, or TBHQ indicated in the abscissa. To minimize the complexity of the figure, the qualifiers *Syn* for synergy and *Add* for additive are the only ones shown over specific bars of the bar graph. Analysis of variance comparison of induced values to controls are statistically significant ($p > 0.01$).

oxidoreductases and the down-regulation of genes involved in TGF-β-signaling pathways.

Arsenic has been reported to modify Ah receptor-dependent induction of gene expression and B[a]P toxicity, although its specific effects are still controversial. Arsenic seems to have a positive interaction with B[a]P on lung tumorigenesis and to function as a cocarcinogen (Ishinishi et al., 1977; Pershagen et al., 1984). In vitro, it partially inhibits ligand-inducible CYP1A1 and CYP1A2 activities, although not the protein levels themselves (Jacobs et al., 1998), but in rats in vivo, it increases inducible CYP1A1 in lung but not in liver or kidney (Falkner et al., 1993; Albores et al., 1995). Previous work from our laboratory found that treatment with sodium arsenite had no effect on the induction of Cyp1a1 mRNA by TCDD, although it increased Nqo1 mRNA levels (Maier et al., 2000). Minor, albeit statistically significant, increases of TCDD-dependent Cyp1a1 mRNA induction were observed by others in Hepa1c1c7 cells pretreated with arsenite (Elbekai and El-Kadi, 2004), who also reported the apparent decrease in the activities of the CYP1A enzymes. On the other hand, work from other authors has shown no change (Vakharia et al., 2001a), a small, not statistically significant decrease (Vakharia et al., 2001b), or a statistically significant reduction of 45% (Bessette et al., 2005) in Cyp1a1 mRNA levels in cells coexposed to AHR-ligands and arsenic. At present, we have no explanation for the diversity of results that have been reported in the literature, including those shown here. Technical differences between less accurate Northern blot determinations compared with the more accurate real-time RT-PCR, or the choice of reference gene in the latter, may explain the discrepancies. Resolution of the ques-

tion would require the concerted effort of all the laboratories affected by these results.

The mechanisms responsible for ligand-independent activation of the Ah receptor are poorly understood. Earlier work with MG-132 showed that proteasome inhibition led to AHR nuclear translocation with (Santiago-Josefat et al., 2001) or without (Davarinos and Pollenz, 1999) a significant effect on gene induction. Similar experiments using a constitutively nuclear AHR found that treatment with the HSP90 ligand geldanamycin resulted in rapid degradation of the receptor but that inhibition of degradation by the proteasome inhibitor allowed geldanamycin to transform the nuclear AHR to form a heterodimer with ARNT that was incapable of stimulating transcription (Lees and Whitelaw, 1999). More recently, ligand-independent AHR activation by MG-132 was found to depend on increases in protein kinase C activity (Santiago-Josefat and Fernandez-Salguero, 2003), a finding consistent with the observation that AHR nuclear translocation is a function of cell density and is regulated by phosphorylation and dephosphorylation events in the AHR nuclear export signal (Ikuta et al., 2004a,b) and possibly in other domains (Minsavage et al., 2004). Arsenite has been shown to inhibit ubiquitin-dependent protein degradation and turnover of ubiquitin-substrate conjugation by inhibiting arginylation of substrate and conjugation of ubiquitin (Klemperer and Pickart, 1989; Kirkpatrick et al., 2003). It is likely that inhibition of ubiquitin-dependent degradation mimics the same effects caused by MG-132 and ultimately leads to AHR nuclear translocation. In this context, it is worth noting that degradation of the nuclear AHR seems to take place initially at a slower rate in arsenite-treated cells compared with TCDD-treated cells (Fig. 3B). On the other hand, arsenite binding to vicinal dithiols in HSP90 has been shown to block its ability to reduce cytochrome c (Nardai et al., 2000), suggesting the possibility that AHR translocation might result from disruption of the molecular interaction between receptor and chaperone. In this context, it is worth noting that our results suggest that HSP90 does not translocate with AHR in arsenite-treated cells, although it does in TCDD-treated cells. These two alternatives are not mutually exclusive and might cooperate to cause the ultimate effect.

Arsenite-induced AHR nuclear translocation was considerably less efficient in transactivation than ligand-induced translocation, even though both induced DNA binding. This difference might be explained by differences in the amount of AHR complex bound in either case (compare the intensity of the lanes in the EMSA data shown in Fig. 3), or by other possible consequences of interactions between arsenite and AHR, ARNT, and any of a number of coregulators and chromatin remodeling factors involved in AHR-dependent transactivation. Nonetheless, cotreatment with arsenite and TCDD in Hepa-1 cells caused a significant additive effect in *Cyp1a1* expression. An additive effect was also evident in MEFs cotreated with low-concentration arsenite and B[a]P, but the effect was lost by 5 μM sodium arsenite, the higher arsenite concentration tested in these cells. In contrast, induction of *Nqo1* by arsenite and B[a]P in both Hepa-1 and MEF cells was synergistic at the two lower concentrations tested (1 and 2 μM) and additive at the higher concentration of 5 μM. Neither additive nor synergistic *Nqo1* induction effects were observed when arsenite was given in combination with

Fig. 8. Arsenite and B[a]P synergy in Nqo1 induction depends on the AHR. MEFs from $Ahr^{+/+}$ and $Ahr^{-/-}$ mice in a C57BL/6J genetic background were treated for 6 h with the concentrations of sodium arsenite, B[a]P, or both indicated in the abscissa. RNA from these cells was used for real-time RT-PCR quantitation of Nqo1 mRNA.

TBHQ, the prototypical inducer of Nrf2-dependent gene expression. *Nqo1* is regulated both by antioxidants (such as TBHQ) and planar polycyclic aromatic hydrocarbons such as (B[*a*]P) (Nioi and Hayes, 2004). The failure of TBHQ and arsenite to synergize suggests that synergy was mediated not by Nrf2 or by generation of oxidative stress by arsenite but more likely by the arsenite effects on the AHR.

Results from global gene expression analyses of cotreatment with arsenite and B[*a*]P point at an effect of either compound and more so of the mixture on the expression of genes in the TGF-β regulatory pathway. TCDD and B[*a*]P have been shown previously to repress TGF-β–regulated genes in an AHR-dependent manner (Gaido et al., 1992; Guo et al., 2004). Down-regulation of TGF-β pathways may have important consequences on the fate of cells or tissues exposed to combined mixtures of B[*a*]P and arsenite. Loss of differentiation or apoptotic directions may force exposed cells in a proliferative direction, which, combined with the promutagenic environment provided by B[*a*]P, may provide initiating as well as a promoting events. We believe that this is a testable hypothesis to explain the co-mutagenic effect of arsenite and B[*a*]P that we have observed in previous experiments (Maier et al., 2002).

References

Albores A, Sinal CJ, Cherian MG, and Bend JR (1995) Selective increase of rat lung cytochrome P450 1A1 dependent monooxygenase activity after acute sodium arsenite administration. *Can J Physiol Pharmacol* **73:**153–158.

Alexander DL, Eltom SE, and Jefcoate CR (1997) Ah receptor regulation of CYP1B1 expression in primary mouse embryo-derived cells. *Cancer Res* **57:**4498–4506.

Andrew AS, Warren AJ, Barchowsky A, Temple KA, Klei L, Soucy NV, O'Hara KA, and Hamilton JW (2003) Genomic and proteomic profiling of responses to toxic metals in human lung cells. *Environ Health Perspect* **111:**825–835.

Barker CW, Fagan JB, and Pasco DS (1994) Down-regulation of P4501A1 and P4501A2 mRNA expression in isolated hepatocytes by oxidative stress. *J Biol Chem* **269:**3985–3990.

Benjamini Y and Hochberg Y (1995) Controlling the false discovery rate: a practical and powerful approach to multiple testing. *J R Stat Soc B* **57:**289–300.

Bernhard HP, Darlington GJ, and Ruddle FH (1973) Expression of liver phenotypes in cultured mouse hepatoma. *Dev Biol* **35:**83–96.

Bessette EE, Fasco MJ, Pentecost BT, and Kaminsky LS (2005) Mechanisms of arsenite-mediated decreases in benzo[k]fluoranthene-induced human cytochrome P4501A1 levels in HepG2 cells. *Drug Metab Dispos* **33:**312–320.

Davarinos NA and Pollenz RS (1999) Aryl hydrocarbon receptor imported into the nucleus following ligand binding is rapidly degraded via the cytoplasmic proteasome following nuclear export. *J Biol Chem* **274:**28708–28715.

Denison MS, Vella LM, and Okey AB (1987) Structure and function of the Ah receptor: sulfhydryl groups required for binding of 2,3,7,8-tetrachlorodibenzo-*p*-dioxin to cytosolic receptor from rodent livers. *Arch Biochem Biophys* **252:**388–395.

DeRisi J, Penland L, Brown PO, Bittner ML, Meltzer PS, Ray M, Chen Y, Su YA, and Trent JM (1996) Use of a cDNA microarray to analyse gene expression patterns in human cancer. *Nat Genet* **14:**457–460.

Dudoit S, Yang YH, Callow MJ, and Speed TP (2002) Statistical methods for identifying differentially expressed genes in replicated cDNA microarray experiments. *Stat Sinica* **12:**111–139.

Elbekai RH and El-Kadi AO (2004) Modulation of aryl hydrocarbon receptor-regulated gene expression by arsenite, cadmium, and chromium. *Toxicology* **202:**249–269.

Falkner KC, McCallum GP, and Bend JR (1993) Effects of arsenite treatment on NAD(P)H:Quinone acceptor oxidoreductase activity in liver, lung, kidney and heart of the rat. Comparison to induction by the polyaromatic hydrocarbon, β-naphthoflavone. *Drug Metab Dispos* **21:**334–337.

Fernandez-Salguero P, Pineau T, Hilbert DM, McPhail T, Lee SS, Kimura S, Nebert DW, Rudikoff S, Ward JM, and Gonzalez FJ (1995) Immune system impairment and hepatic fibrosis in mice lacking the dioxin-binding Ah receptor. *Science (Wash DC)* **268:**722–726.

Gaido KW, Maness SC, Leonard LS and Greenlee WF (1992) 2,3,7,8-Tetrachlorodibenzo-*p*-dioxin-dependent regulation of transforming growth factors-α and -β2 expression in a human keratinocyte cell line involves both transcriptional and post-transcriptional control. *J Biol Chem* **267:**24591–24595.

Guo J, Sartor M, Karyala S, Medvedovic M, Kann S, Puga A, Ryan P, and Tomlinson CR (2004) Expression of genes in the TGF-beta signaling pathway is significantly deregulated in smooth muscle cells from aorta of aryl hydrocarbon receptor knockout mice. *Toxicol Appl Pharmacol* **194:**79–89.

Ikuta T, Kobayashi Y, and Kawajiri K (2004a) Cell density regulates intracellular localization of aryl hydrocarbon receptor. *J Biol Chem* **279:**19209–19216.

Ikuta T, Kobayashi Y, and Kawajiri K (2004b) Phosphorylation of nuclear localization signal inhibits the ligand-dependent nuclear import of aryl hydrocarbon receptor. *Biochem Biophys Res Commun* **317:**545–550.

Ireland RC, Li SY, and Dougherty JJ (1995) The DNA binding of purified ah receptor heterodimer is regulated by redox conditions. *Arch Biochem Biophys* **319:**470–480.

Ishinishi N, Kodama Y, Nobutomo K, and Hisanaga A (1977) Preliminary experimental study on carcinogenicity of arsenic trioxide in rat lung. *Environ Health Perspect* **19:**191–196.

Jacobs J, Roussel R, Roberts M, Marek D, Wood S, Walton H, Dwyer B, Sinclair P, and Sinclair J (1998) Effect of arsenite on induction of cyp1a and cyp2h in primary cultures of chick hepatocytes. *Toxicol Appl Pharmacol* **150:**376–382.

Kapahi P, Takahashi T, Natoli G, Adams SR, Chen Y, Tsien RY, and Karin M (2000) Inhibition of NF-κB activation by arsenite through reaction with a critical cysteine in the activation loop of IκB kinase. *J Biol Chem* **275:**36062–36066.

Kester JE and Gasiewicz TA (1987) Characterization of the in vitro stability of the rat hepatic receptor for 2,3,7,8-tetrachlorodibenzo-*p*-dioxin (TCDD). *Arch Biochem Biophys* **252:**606–625.

Kirkpatrick DS, Dale KV, Catania JM, and Gandolfi AJ (2003) Low-level arsenite causes accumulation of ubiquitinated proteins in rabbit renal cortical slices and HEK293 cells. *Toxicol Appl Pharmacol* **186:**101–109.

Klemperer NS and Pickart CM (1989) Arsenite inhibits two steps in the ubiquitin-dependent proteolytic pathway. *J Biol Chem* **264:**19245–19252.

Lees MJ and Whitelaw ML (1999) Multiple roles of ligand in transforming the dioxin receptor to an active basic helix-loop-helix/PAS transcription factor complex with the nuclear protein Arnt. *Mol Cell Biol* **19:**5811–5822.

Maier A, Dalton TP, and Puga A (2000) Disruption of dioxin-inducible phase i and phase ii gene expression patterns by cadmium, chromium and arsenic. *Mol Carcinog* **28:**225–235.

Maier A, Schumann BL, Chang X, Talaska G, and Puga A (2002) Arsenic co-exposure potentiates benzo[a]pyrene genotoxicity. *Mutat Res* **517:**101–111.

Minsavage GD, Park SK, and Gasiewicz TA (2004) The aryl hydrocarbon receptor (AhR) Tyrosine 9, a residue that is essential for AhR DNA binding activity, is not a phosphoresidue but augments ahr phosphorylation. *J Biol Chem* **279:**20582–20593.

Morel Y and Barouki R (1998) Down-regulation of cytochrome P450 1A1 gene promoter by oxidative stress. Critical contribution of nuclear factor 1. *J Biol Chem* **273:**26969–26976.

Nardai G, Sass B, Eber J, Orosz G, and Csermely P (2000) Reactive cysteines of the 90-kda heat shock protein, Hsp90. *Arch Biochem Biophys* **384:**59–67.

Nazarenko DA, Dertinger SD, and Gasiewicz TA (2001) In vivo antagonism of AhR-mediated gene induction by 3′-methoxy-4′-nitroflavone in TCDD-responsive LacZ Mice12. *Toxicol Sci* **61:**256–264.

Nieboer E and Fletcher GG (1996) Determinants of reactivity in metal toxicology, in *Toxicology of Metals*, pp 113–132, CRC Press, Boca Raton, FL.

Nioi P and Hayes JD (2004) Contribution of NAD(P)H:quinone oxidoreductase 1 to protection against carcinogenesis and regulation of its gene by the Nrf2 basic-region leucine zipper and the arylhydrocarbon receptor basic helix-loop-helix transcription factors. *Mutat Res* **555:**149–171.

Pershagen G, Nordberg G, and Bjorklund NE (1984) Carcinomas of the respiratory tract in hamsters given arsenic trioxide and/or benzo[a]pyrene by the pulmonary route. *Environ Res* **34:**227–241.

Pollenz RS (2002) The mechanism of AH receptor protein down-regulation (degradation) and its impact on AH receptor-mediated gene regulation. *Chem Biol Interact* **141:**41–61.

Puga A, Barnes SJ, Chang C, Zhu H, Nephew KP, Khan SA, and Shertzer HG (2000) Activation of transcription factors activator protein-1 and nuclear factor-kappaB by 2,3,7,8-tetrachlorodibenzo-*p*-dioxin. *Biochem Pharmacol* **59:**997–1005.

Rea MA, Gregg JP, Qin Q, Phillips MA, and Rice RH (2003) Global alteration of gene expression in human keratinocytes by inorganic arsenic. *Carcinogenesis* **24:**747–756.

Reiner A, Yekutieli D, and Benjamini Y (2003) Identifying differentially expressed genes using false discovery rate controlling procedures. *Bioinformatics* **19:**368–375.

Roussel RR and Barchowsky A (2000) Arsenic inhibits NF-kappaB-mediated gene transcription by blocking IkappaB kinase activity and IkappaBalpha phosphorylation and degradation. *Arch Biochem Biophys* **377:**204–212.

Santiago-Josefat B and Fernandez-Salguero PM (2003) Proteasome inhibition induces nuclear translocation of the dioxin receptor through an Sp1 and protein kinase C-dependent pathway. *J Mol Biol* **333:**249–260.

Santiago-Josefat B, Pozo-Guisado E, Mulero-Navarro S, and Fernandez-Salguero PM (2001) Proteasome inhibition induces nuclear translocation and transcriptional activation of the dioxin receptor in mouse embryo primary fibroblasts in the absence of xenobiotics. *Mol Cell Biol* **21:**1700–1709.

Stohs SJ and Bagchi D (1995) Oxidative mechanisms in the toxicity of metal ions. *Free Radic Biol Med* **18:**321–336.

Tan Z, Chang X, Puga A, and Xia Y (2002) Activation of mitogen-activated protein kinases (MAPKs) by aromatic hydrocarbons: role in the regulation of aryl hydrocarbon (AHR) function. *Biochem Pharmacol* **64:**771–780.

Tinwell H, Stephens SC, and Ashby J (1991) Arsenite as the probable active species in the human carcinogenicity of arsenic: mouse micronucleus assays on Na and K arsenite, orpiment and Fowler's solution. *Environ Health Perspect* **95:**205–210.

Vakharia DD, Liu N, Pause R, Fasco M, Bessette E, Zhang QY, and Kaminsky LS

(2001a) Effect of metals on polycyclic aromatic hydrocarbon induction of CYP1A1 and CYP1A2 in human hepatocyte cultures. *Toxicol Appl Pharmacol* **170:**93–103.

Vakharia DD, Liu N, Pause R, Fasco M, Bessette E, Zhang QY, and Kaminsky LS (2001b) Polycyclic aromatic hydrocarbon/metal mixtures: effect on PAH induction of CYP1A1 in human HEPG2 cells. *Drug Metab Dispos* **29:**999–1006.

Wang Z and Rossman TG (1996) The carcinogenicity of arsenic, in *Toxicology of Metals*, pp 221–229, CRC Press, Boca Raton, FL.

Wolfinger RD, Gibson G, Wolfinger ED, Bennett L, Hamadeh H, Bushel P, Afshari C, and Paules RS (2001) Assessing gene significance from CDNA microarray expression data via mixed models. *J Comput Biol* **8:**625–637.

Xu C and Pasco DS (1998) Suppression of CYP1A1 transcription by H_2O_2 is mediated by xenobiotic-response element. *Arch Biochem Biophys* **356:**142–150.

Address correspondence to: Alvaro Puga, Department of Environmental Health, University of Cincinnati Medical Center, P.O. Box 670056, Cincinnati, OH 45367-00567. E-mail: alvaro.puga@uc.edu